UNIVERSITY OF CALIFORNIA, SAN DIEGO

Viral Transduction of Human Cancer Cell Lines with an Optimized Triple Modality Reporter for Quantifiable Tumor Imaging and Therapy Evaluation *In Vivo*

A thesis submitted in partial satisfaction of the
requirements for the degree Master of Science
in
Biology

by

Rachel Ashley Levin

Committee in charge:

Professor Quyen Nguyen, Chair
Professor James Kadonaga, Co-Chair
Professor Roger Tsien
Professor Dong-Er Zhang

2013

The thesis of Rachel Ashley Levin is approved, and it is acceptable in quality and form for publication on microfilm and electronically:

_____

_____

_____

Co-Chair

_____

Chair

University of California, San Diego

2013

I dedicate this thesis to my mom for her continuous love and support.

Table of Contents

List of Figures

List of Tables

Acknowledgements

I would first like to thank Dr. Quyen Nguyen for serving as my Thesis Chair and for supporting me in the project presented in this thesis as well as in several other projects not included in this document.

Next, I would like to express my appreciation to Dr. Roger Tsien for giving me the opportunity to join his lab and for advising me in this project. Over the past three and a half years in the Tsien lab, I have grown tremendously as a scientist and have been inspired to move forward beyond this degree to pursue my research passions outside of this lab.

I would like to thank Csilla Felsen for generously training me in techniques required for succeeding in this project and for being a great mentor and friend to me every step along the way. Also, I would like to recognize Jin Yang for initially cloning the optimized triple modality reporter construct.

I would like to thank Dr. James Kadonaga for giving me my first academic research internship four years ago in his lab, as well as for serving as my Thesis Co-Chair.

Additionally, I would like to thank both Dr. Roger Tsien and Dr. Dong-Er Zhang for serving as members of my thesis committee.

Lastly, I would like to thank all the members of the Tsien lab and my friends and family for their encouragement and support as I worked towards this graduate degree.

ABSTRACT OF THE THESIS

Viral Transduction of Human Cancer Cell Lines with an Optimized Triple Modality Reporter for Quantifiable Tumor Imaging and Therapy Evaluation *In Vivo*

by

Rachel Ashley Levin

Master of Science in Biology

University of California, San Diego, 2013

Professor Quyen Nguyen, Chair

Professor James Kadonaga, Co-Chair

This thesis presents an optimized triple modality reporter combining genes for a far-red fluorescent protein (E2-Crimson), enhanced firefly luciferase enzyme (Luc2), and truncated wild type herpes simplex virus I thymidine kinase (wttk). This schematic allows for sensitive, long-term tracking of tumor growth *in vivo* by fluorescence, bioluminescence, and positron emission tomography. This triple reporter improves on previous designs in three ways. 1) The shorter wavelength green fluorescent protein (GFP) or monomeric red fluorescent protein (mRFP1) has been replaced with E2-

Crimson to increase penetration of fluorescence signal through mammalian tissues. 2) Firefly luciferase (fLuc), *Renilla* luciferase (hrl), or mutant thermally stable firefly luciferase (mtfl) has been replaced by Luc2, a codon optimized firefly luciferase for increased expression in mammalian cells and detection of single cells by bioluminescence. 3) Self-cleaving viral 2A sequences separate each component, ensuring equal stoichiometry of the reporter genes without requiring protein fusion or the use of internal ribosomal entry site (IRES) sequences. Cleavage between each protein gene product allows for proper protein folding, trafficking, and full activity of each modality. This optimized triple reporter construct was cloned into a second-generation lentiviral vector, and a lentivirus was produced. Two human cancer cell lines were virally transduced with the triple reporter construct, and expression of all three modalities was confirmed in both cell lines *in vitro* and *in vivo*. Finally, the therapeutic responses of the MDA231 human breast cancer cell line to the chemotherapeutic agents monomethyl auristatin E (MMAE) and monomethyl auristatin F (MMAF) were successfully quantified *in vivo* by optical imaging of the optimized triple modality reporter. This is the first reported use of both fluorescence and bioluminescence signals from a multi-reporter construct to measure drug efficacy *in vivo*.

I:

Introduction

Background

The development of noninvasive imaging technologies is significantly advancing the field of molecular imaging. Molecular imaging includes nonradionuclide technologies, such as fluorescence and bioluminescence optical imaging, and radionuclide technologies, such as positron emission tomography (PET). Molecular imaging is commonly used to analyze the molecular pathways of cancer initiation, cancer growth, and therapy responses in living subjects (*1*). However each molecular imaging modality has benefits and shortcomings. By combining a fluorescent protein gene for fluorescence imaging, a luciferase gene for bioluminescence imaging, and a thymidine kinase gene for PET into one construct, all the advantages of each imaging modality are made available, while eliminating the disadvantages of each modality when otherwise used alone.

Fluorescence Imaging

The first component in this optimized triple modality reporter is the fluorescent protein E2-crimson for fluorescence imaging. Fluorescent proteins are ~25 kDa in size with structures consisting of a central alpha-helix, which forms the chromophore, surrounded by an extremely rigid beta-barrel (*2*). Visible light hits the chromophore and is absorbed by exciting an electron from its ground state into an excited state. The absorbed energy is then released in the form of a photon as the excited electron falls back down to its ground state (*3*).

The key advantages of fluorescent proteins are that they can be detected in living or dead cells, have high single cell resolution, and do not require a substrate in order to

produce fluorescence signal. For these reasons, fluorescent proteins are essential for fluorescent-activated cell sorting (FACS), determining transduction efficiency by microscopy, and calibrating injectable optical probes such as activatable cell-penetrating peptides (ACPPs). However, short wavelength fluorescence signal has high depth attenuation in mammalian tissue, limiting the use of many fluorescent proteins *in vivo*. For this reason, this optimized triple modality reporter contains the far-red fluorescent protein, E2-Crimson (excitation maximum 611 nm, emission maximum 648 nm), which allows for improved penetration of the fluorescence signal in whole animal live imaging, unlike previous triple reporter designs (*4*-*8*) that have the shorter wavelength eGFP (excitation maximum 488 nm, emission maximum 507 nm) or mRFP (excitation maximum 584 nm, emission maximum 607 nm). Yet, even when using a far-red fluorescent protein, mammalian tissues still have high levels of autofluorescence that can make the tumor boundaries unclear.

Bioluminescence Imaging

The second gene in this triple reporter is enhanced firefly luciferase (Luc2). Bioluminescence is produced when firefly luciferase catalyzes a reaction involving D-luciferin and ATP, producing luciferyl adenylate. When luciferyl adenylate reacts with oxygen, it forms oxyluciferin in an electronically excited state. As oxyluciferin returns to the ground state, it releases a photon of light. Nearly 90% of the energy added to the reaction is transformed into light with a peak emission wavelength around 560 nm (*9*). Due to this highly efficient reaction, luciferase signal has greater sensitivity and better depth penetration than fluorescent protein signal, despite its shorter emission wavelength.

Another benefit is that tissues lack significant background bioluminescence signal, but unlike the fluorescence signal from fluorescent proteins, luciferase only produces signal after the injection of an external substrate.

Luc2 is a codon-optimized luciferase engineered to have increased expression in mammalian cells (*10*). Because of this enhancement, it has been shown to detect single cancer cells *in vivo* by bioluminescence unlike fLuc, hrl, and mtfl, which have been used in previous triple reporters (*4-8*). However, while Luc2 can be used to detect single cells, it still has poor single cell resolution compared to fluorescent proteins.

Positron Emission Tomography

The last of the three reporter genes in this triple reporter is truncated wild type HSV-1 thymidine kinase (wttk), which allows for PET. PET imaging of the reporter gene expression requires radiolabelled probes that are selectively metabolized by a specific enzyme, resulting in a radiolabelled product that is trapped in the cell. To image tumors with the wttk transgene, the radiolabelled probe 9-(4-18F-fluoro-3-[hydroxymethyl]butyl)guanine, referred to as 18F-FHBG, is intravenously administered to live animals then transported into cells. Wttk phosphorylates 18F-FHBG in the labeled cancer cells, making it difficult for 18F-FHBG to travel back across the cell membrane and exit the cell. This causes an accumulation of 18F-FHBG in cells expressing wttk, increasing their PET signal (*11*).

The use of wttk in microPET experiments with live animals can produce three-dimensional images, and PET signal has better depth penetration than fluorescence signal and bioluminescence signal. However, PET has the poorest cellular resolution of the

three reporters, making the quantification of PET signal in small tumors less reliable. Also, like Luc2, wttk requires the administration of an external substrate to produce signal. Finally, the radioactive substrate and equipment required for PET imaging is costly and has higher safety risks than fluorescence and bioluminescence optical imaging.

Self-Cleaving Viral 2A Sequence

When designing this triple reporter, a major concern was how to combine the three modalities to allow for equal reporter gene stoichiometry while avoiding protein fusion. Large fusions of several reporter proteins may affect protein folding and/or trafficking, consequently reducing protein activity (*7, 8*). A common strategy to avoid large protein fusions is the use of internal ribosomal entry sites (IRES). In most eukaryotes, translation is initiated by recognition of the 5' cap of the mRNA. Conversely, in viral systems, translation of mRNA occurs in a cap-independent matter based on IRES (*12*). Since their initial discovery in viruses, IRES sequences have been identified in many eukaryotes including *Drosophila* and higher eukaryotes. The placement of IRES sequences linking genes in multi-reporters allows for equal stoichiometry of the transduced genes. Unfortunately, in most cases, the translation efficiency of the 5' cap and the IRES are not equal, leading to a significant imbalance in gene expression (*13*).

Instead, self-cleaving viral 2A sequences are utilized in this optimized triple reporter construct. The cleavage of the 2A sequence does not involve proteases, but rather, translation is disrupted by damage to the bond between the last glycine residue and first proline residue on the C-terminus of the highly conserved consensus motif: D-

X-E-X-N-P-G-P. Cleavage of the 2A sequence does not affect the translation of the downstream protein sequence(s). The mRNA bond modification prevents nucleophilic attack of the incoming tRNA nitrogen residue required to create a peptide bond between the glycine and proline: D-X-E-X-N-P-G-cleavage-P (*14*). 2A peptide sequences were chosen for this triple reporter because they are small and allow for strong expression of downstream genes regardless of their order in the construct unlike IRES (*13*). Therefore, this optimized triple reporter containing viral 2A sequences improves on previous triple reporter designs by ensuring equal molarity of reporter genes without requiring protein fusion or the use of IRES (*4-7*).

The 2A sequences used in this triple reporter are from porcine teschovirus-1 (located between E2-Crimson and Luc2) and thosea asigna virus (located between Luc2 and wttk). The 2A porcine teschovirus-1 2A sequence (ATNFSLLKQAGDVEENPGP) is referred to as P2A, and the thosea asigna virus 2A sequence (EGRGSLLTCGDVEENPGP) is referred to as T2A. A GSG linker (GGGSGGG) precedes each 2A peptide to separate the 2A peptide from the upstream reporter, which prevents the 2A peptide from interfering with independent protein folding of the reporter gene product after self-cleavage.

Viral Transduction of Human Cancer Cell Lines with the Triple Reporter

Initially, this triple reporter was inserted into the pcDNA3.1/hygro+ vector using the multiple cloning site located downstream from the hygromycin resistance gene. The resulting plasmid was transfected into cancer cell lines in culture. The cell lines were treated with hygromycin B for one month to promote integration of the plasmid

containing the triple reporter construct into the genomic DNA of the cells. However, due to selection against the energetically costly triple reporter construct, it was observed that the cell lines stably expressed the hygromycin resistance gene, but failed to incorporate one or more of the reporter genes into their genome. Due to this problem with plasmid transfection, the triple reporter construct was cloned into a second-generation lentiviral plasmid.

The second-generation lentiviral vector, package plasmid, and envelope plasmid necessary for lentivirus production were derived from the HIV-1 genome. HIV-1 derived lentiviruses can efficiently infect and express their genes in human cells. They can infect both dividing and nondividing cells because their preintegration complex crosses the intact membrane of the nucleus in the target cell without requiring initiation of mitosis (*15*). The lentivirus genome is flanked by long terminal repeating sequences (LTRs) that are essential to the virus life cycle. Once the preintegration complex enters the nucleus of a target cell, the viral RNA located between the LTRs is reverse transcribed into DNA and inserted directly into the cell's genomic DNA, which allows for reliable, long-term expression of foreign genes (*16, 17*). Also, by using a high titer lentivirus, multiple viruses can infect a single cell, giving each cell multiple copies of the gene of interest (*18*). Transduction of multiple gene copies can increase the expression of each transduced gene as well as protect against mutations that could eliminate expression of the gene.

After cloning the triple reporter construct into the lentiviral plasmid, a high titer lentivirus was produced and used to successfully transduce the triple reporter construct

into the MDA231 human breast cancer cell line and the HT1080 human fibrosarcoma cell line.

Quantifying Therapeutic Effect with the Triple Reporter *in vivo*

Monomethyl auristatin E (MMAE) and monomethyl auristatin F (MMAF) are antimitotic drugs that inhibit tubulin polymerization and may also damage the intratumoral vasculature (*19*). MMAF was designed to be significantly less potent than MMAE when untargeted to tumors and administered as a free drug because of a charged phenylalanine residue on the C-terminus of MMAF that impairs its intracellular access (*20*). However, MMAF can be conjugated to a monoclonal antibody and delivered to tumors to increase its potency >2200-fold *in vitro (20, 21)*. In this thesis, the therapeutic effects of unconjugated MMAE and MMAF on breast cancer tumors were quantified based on optical signal of the optimized triple modality reporter in the MDA231 cell line. This is the first reported evaluation of drug efficacy by multi-reporter construct fluorescence and bioluminescence imaging *in vivo*.

II:
Results

Construction of Triple Reporter Cell Lines

Jin Yang, a laboratory technician in the Tsien lab, initially cloned the triple reporter construct into the pcDNA3.1/hygro+ vector. Trono Lab at Ecole Polytechnique Fédérale de Lausanne provided the second-generation lentiviral vector, psPAX2 lentiviral packaging plasmid, and pMDG.2 envelope plasmid.

The BamHI restriction site between the Luc2 and wttk genes in the pcDNA3.1/hygro+ vector was successfully mutated through site directed mutagenesis. The resulting vector was amplified through transformation of chemically competent cells and purified. The EcoRI restriction site was added to the 5' end of the triple reporter construct, and the BamHI restriction site was added to the 3' end of the triple reporter construct by PCR primers. The PCR product was confirmed through gel electrophoresis, and the triple reporter construct with the additional restriction sites was gel purified. The triple reporter construct and the lentiviral vector were digested by EcoRI and BamHI high fidelity restriction enzymes. The cut lentiviral vector was dephosphorylated and ligated with the cut triple reporter insert to form the triple reporter lentiviral plasmid (Figure 1). The triple reporter lentiviral plasmid, psPAX2 lentiviral packaging plasmid, and pMDG.2 envelope plasmid were transiently transfected into the HEK293A packaging cell line to produce the triple reporter lentivirus. This lentivirus was used to transduce wild type MDA231 cells and wild type HT1080 cells with the triple reporter construct.

***In Vitro* Expression of Each Triple Reporter Modality**

Three weeks after transduction, stable expression of E2-Crimson was observed in both cell lines. Each cell line was fluorescent-activated cell sorted (FACS) for the

brightest 1.5% of cells expressing E2-Crimson with a 568 nm excitation laser and 660/20 nm emission filter at 100 mW (Figure 2a). The FACS populations of each cell line were grown in culture for three weeks and then imaged with an epifluorescence microscope with a 580/20 nm excitation filter and a 653/95 nm emission filter on the 40x oil objective (Figure 2b).

Next, the cell lines were tested for Luc2 activity. 7.4×10^4 cells from each cell line were seeded in each well of a 48 well tissue culture plate in triplicate. After 24 hours, the cells were bathed in a 150 μg/ml solution of D-luciferin and immediately imaged using an IVIS Spectrum (FOV; C, binning; medium, f stop; 1, exposure time; auto) (Figure 3). The MDA231 triple reporter FACS population had an average bioluminescence signal of $7.10 \times 10^8 \pm 1.92 \times 10^7$ per well *in vitro*. The HT1080 triple reporter FACS population had an average bioluminescence signal of $9.30 \times 10^8 \pm 2.96 \times 10^7$ per well *in vitro*. The MDA231 wild type population and HT1080 wild type population showed no significant bioluminescence signal.

Thirdly, the cell lines were tested for wttk activity, which was accomplished by measuring each cell line's sensitivity to ganciclovir. The ganciclovir nucleoside prodrug can be enzymatically phosphorylated to an active triphosphate analog by wttk. The phosphorylated product causes inhibition of DNA polymerase, resulting in cell death (*22*). 4×10^3 cells of each cell line were treated with 0 μg/ml, 1 μg/ml, or 10 μg/ml of ganciclovir in triplicate. After six days of ganciclovir exposure, cell death was quantified (Figure 4). Both of the triple reporter FACS populations were significantly more sensitive to ganciclovir treatment at 1 μg/ml and 10 μg/ml than the wild type cell populations. The MDA231 triple reporter FACS population was significantly more

sensitive to ganciclovir treatment at 1 μg/ml and 10 μg/ml than the HT1080 triple reporter FACS population.

Self-Cleavage of the Viral 2A Sequences

Finally, successful self-cleavage of the viral 2A sequences was confirmed by Western blot (Figure 5). A fusion protein consisting of all three modalities has an expected molecular weight of 135 kDa. A band of this molecular weight was not detected by any of the primary antibodies. E2-Crimson with an attached GSG linker and viral 2A sequence has an expected MW of 29 kDa. The detected E2-Crimson band ran around 24 kDa. The reason for the lower MW is unknown. Luc2 with an attached GSG linker and viral 2A sequence has an expected MW of 66 kDa. The detected Luc2 band ran around 66 kDa. Wttk has an expected MW of 40 kDa. The detected wttk band ran around 42 kDa. The loading control, GAPDH, has an expected MW of 36 kDa and ran at 36 kDa. The Western blot also confirmed higher expression of wttk in the MDA231 triple reporter FACS population relative to the HT1080 triple reporter FACS population.

***In Vivo* Expression of Each Triple Reporter Modality**

MDA231 triple reporter FACS tumors were grown orthotopically in four female nu/nu mice with two tumors per mouse. HT1080 triple reporter FACS tumors were grown subcutaneously in four female nu/nu mice with two tumors per mouse. As controls, MDA231 wild type tumors were grown orthotopically in two female nu/nu mice with two tumors per mouse, and HT1080 wild type tumors were grown subcutaneously in two female nu/nu mice with two tumors per mouse. High gut retention is characteristic

of 18F-FHBG, requiring that tumors be placed away from the abdomen of each mouse. All tumors were grown for two weeks before imaging.

No significant changes in the growth pattern were observed between the MDA231 triple reporter FACS tumors and MDA231 wild type tumors. No significant changes in growth pattern were observed between the HT1080 triple reporter FACS tumors and HT1080 wild type tumors. Overall, the MDA231 tumors had more uniform growth than the HT1080 tumors.

Each tumor was imaged for fluorescence signal, bioluminescence signal, and PET signal. The whole body fluorescence and bioluminescence signals of each mouse were quantified using Living Image software. PET signal was quantified using AMIDE software. For quantifying PET, the % bioavailable dose of 18F-FHBG in each tumor was calculated by dividing the number of counts in the tumor region by the number of counts in the whole body region. Background fluorescence signal and background PET signal were subtracted from the fluorescence signal and PET signal respectively in the triple reporter tumors. No significant background bioluminescence signal was observed. Representative mice with triple reporter FACS tumors are shown expressing each modality *in vivo* (Figure 6). The coronal plane is shown for PET-CT images.

All eight MDA231 triple reporter FACS tumors were healthy and detectable by all three modalities. Two HT1080 triple reporter FACS tumors were healthy and detectable by all three modalities. Despite the significantly larger size of the HT1080 triple reporter FACS tumors that were detectable by all three modalities, the average PET signal (% bioavailable dose) of the HT1080 triple reporter FACS tumors was not significantly higher than that of the MDA231 triple reporter FACS tumors (Table 1).

One additional large HT1080 triple reporter FACS tumor was detectable by all three modalities, but it was excluded from the data set because it appeared to be partially necrotic based on visual observation of a dark area on the surface of the tumor. Bioluminescence and PET imaging confirmed the necrosis (Figure 7). This tumor was measured to be 587.29 mm^3 by PET-CT and 526.50 mm^3 by caliper measurement. It was significantly larger than the healthy HT1080 triple reporter FACS tumors that were expressing all three modalities, but it had a significantly reduced bioluminescence signal of 1.70×10^{10} (p/s) and a significantly lower PET signal of 4.53×10^{-2} % bioavailable dose. This tumor did not have a significant decrease in fluorescence signal. Total radiant efficiency of this tumor was 3.76×10^9 (p/s)/(cm^2/sr).

Five HT1080 triple reporter FACS tumors were detectable by fluorescence and bioluminescence signals but were not detectable by PET signal. Because they were not detectable by all three modalities *in vivo*, they were excluded from the data set. These tumors were significantly smaller than the healthy HT1080 triple reporter FACS tumors that were expressing all three modalities. These tumors had an average size of 83.50 ± 96.20 mm^3 based on by caliper measurements. They had total fluorescence radiant efficiency of $3.31 \times 10^8 \pm 5.01 \times 10^8$ (p/s)/(cm^2/sr) and an average total bioluminescence radiance photons of $3.04 \times 10^9 \pm 6.10 \times 10^9$ (p/s).

The MDA231 triple reporter FACS population was chosen for use in the MMAE and MMAF therapy experiment because it showed uniform growth *in vivo* and small tumors were detectable by all three modalities.

Quantifying Therapeutic Effect with the Triple Reporter *in vivo*

Two MDA231 triple reporter FACS tumors were grown orthotopically and bilaterally in the mammary fat pads of each five-week old female nu/nu mouse. After seven days of growth, mice were randomized into three groups of five mice, which were untreated, MMAE, and MMAF. The only difference between the structures of MMAE and MMAF is the additional negatively charged residue on MMAF (Figure 8). Starting on day seven, mice in the MMAE and MMAF groups were treated every three days with a dose of 0.5 nmol/g (Figure 9). Tumors were too small to be reliably measured by calipers on day seven. After three doses of MMAE, there was a significant decrease in the fluorescence signal compared to the untreated group. After four doses of MMAE, there was a significant decrease in the bioluminescence signal compared to the untreated group. Six treatments of MMAF at 0.5 nmol/g did not produce a significant decrease in the fluorescence or bioluminescence signal compared to the untreated group. All mice gained weight throughout the experiment. PET signal was not used to monitor tumor growth because there was no access to the necessary equipment. Even with the necessary equipment, it would be logistically difficult to measure PET signal every three days because 18F-FBGH needs to be synthesized the same day it is used, and once injected, it needs to circulate for two hours in each mouse before imaging.

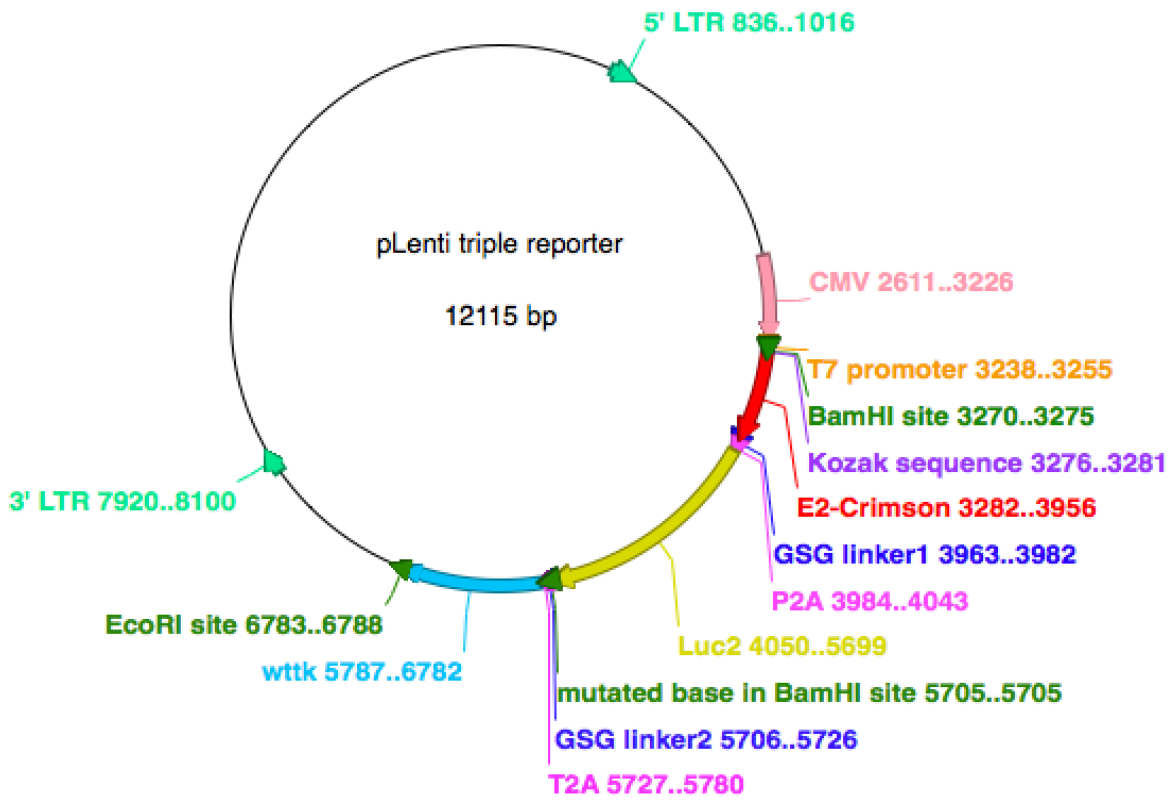

Figure 1. Triple Modality Reporter Lentiviral Plasmid Map

MDA231 and HT1080 human cancer cell lines were virally transduced with the genes placed between the 5' LTR and 3' LTR of this plasmid. Graphic made with ApE (Universal) software.

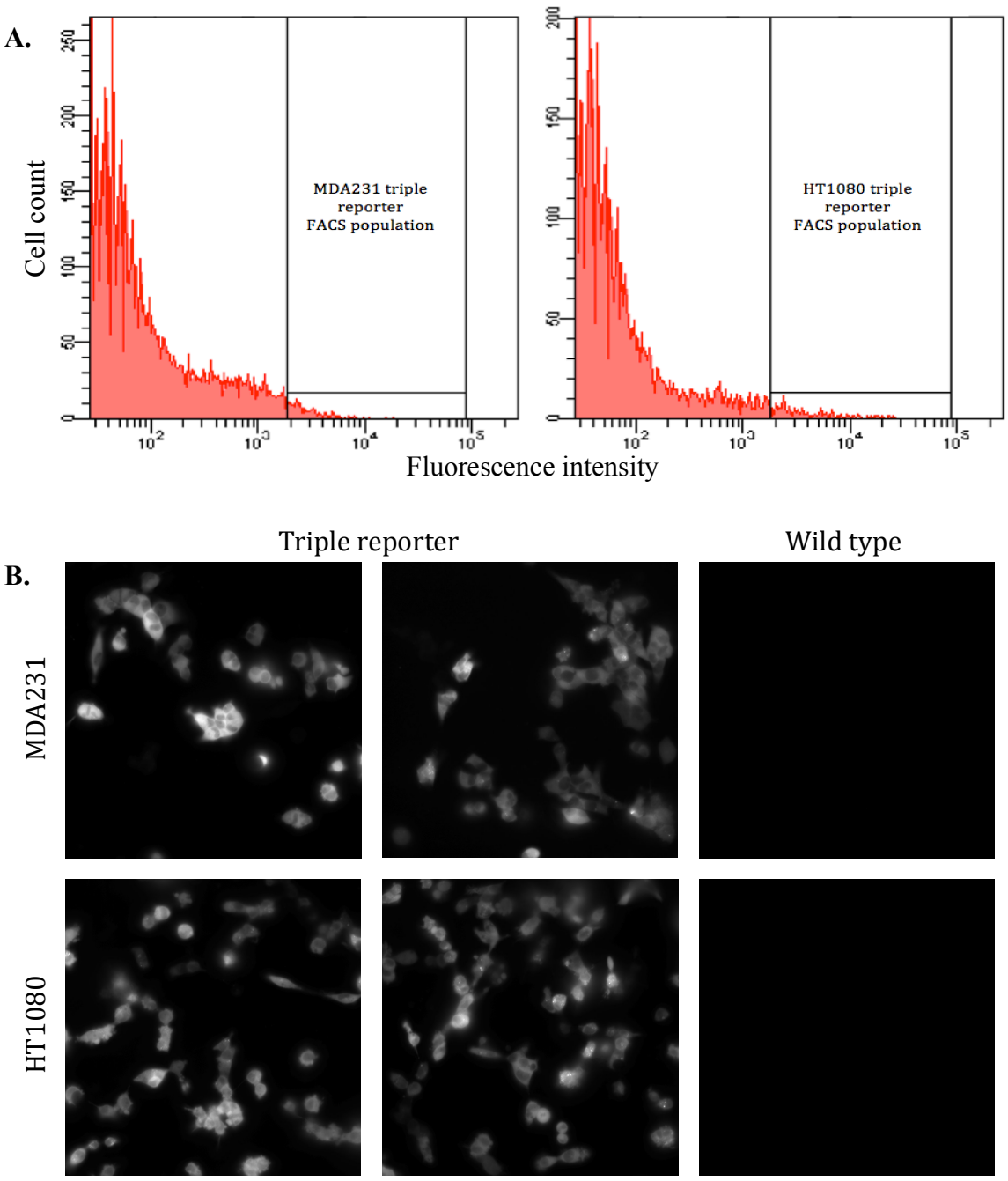

Figure 2. ***In Vitro*** **Expression of E2-Crimson**

(A) The top 1.5% brightest cells in each transduced cell line, based on E2-Crimson, expression were collected through FACS (568 nm excitation laser, 660/20 nm emission filter, 100 mW power).
(B) Epifluorescence microscopy (580/20 nm excitation filter, 653/95 nm emission filter, 1 second exposure, 40x oil objective) of the triple reporter FACS populations compared to the respective wild type cell lines. Images were scaled equally using ImageJ software.

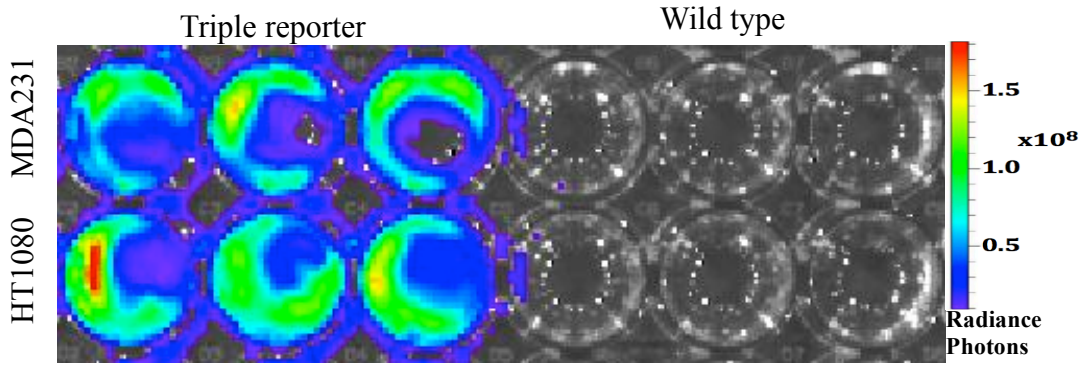

Figure 3. *In Vitro* Activity of Luc2

Bioluminescence signal of the triple reporter FACS populations compared to their respective wild type cell lines immediately after exposure to D-luciferin. The units of the bioluminescence radiance photons are p/s/cm^2/sr.

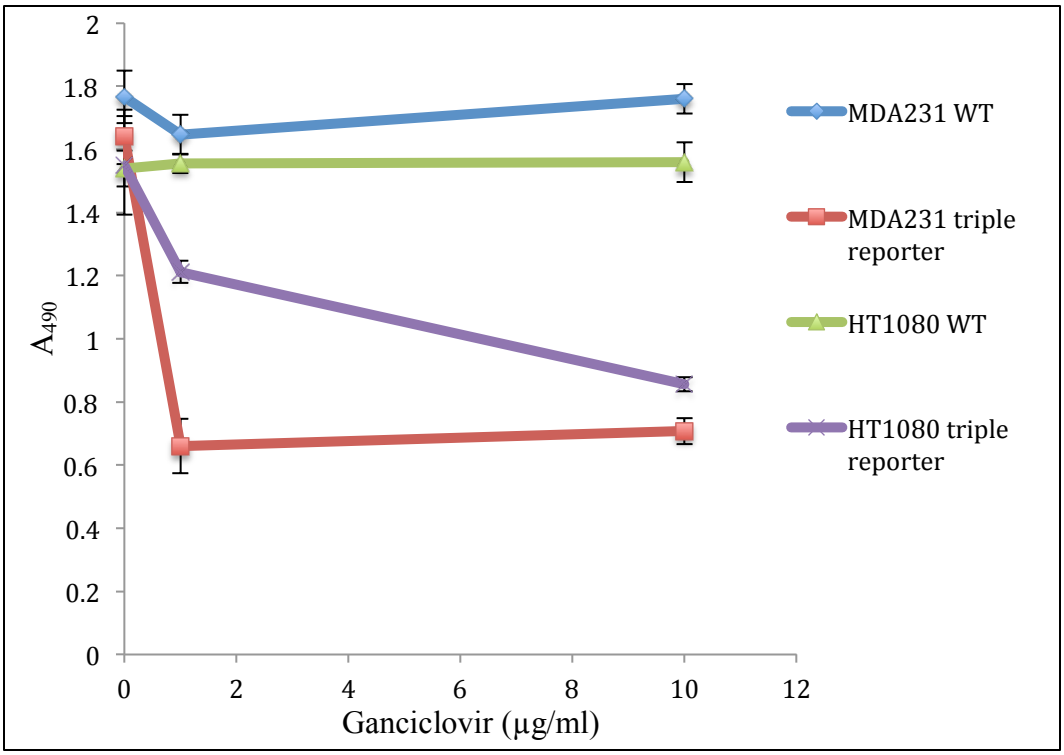

Figure 4. *In Vitro* Activity of Wttk

Wttk activity was measured by cell death after six days of ganciclovir treatment for the triple reporter FACS populations compared to their respective wild type cell lines. Only living cells can convert the CellTiter 96® AQueous One Solution into a product with an absorbance at 490 nm.

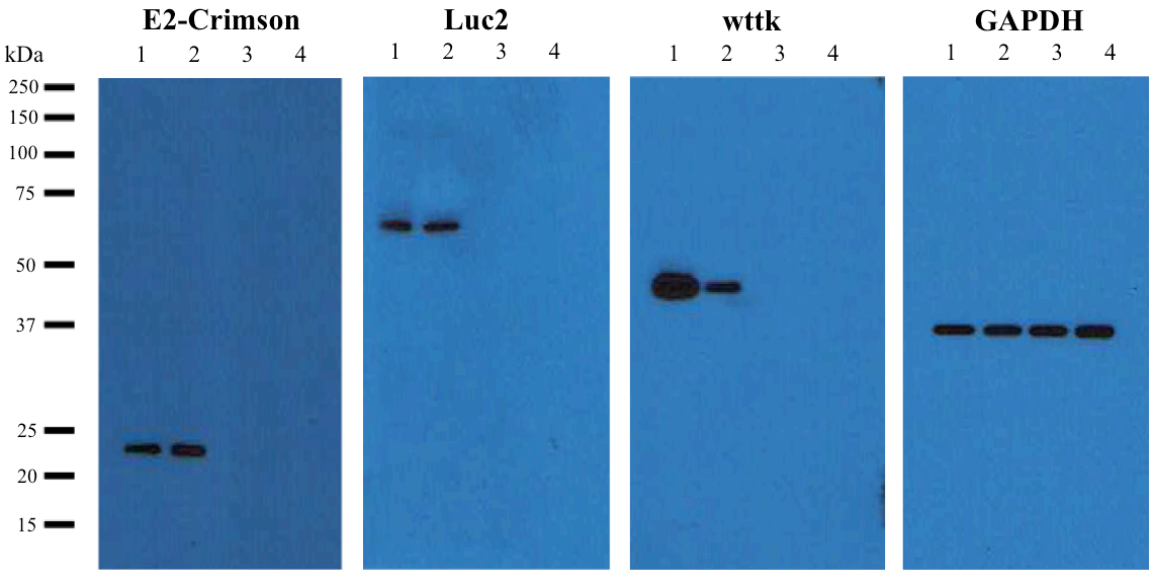

Figure 5. Self-Cleavage of Viral 2A Sequences

Western blots detect the expression of each individual reporter gene in the triple reporter FACS populations and their respective wild type cell lines. GAPDH expression was detected as a loading control. Lane 1: MDA231 triple reporter, Lane 2: HT1080 triple reporter, Lane 3: MDA231 wild type, Lane 4: HT1080 wild type.

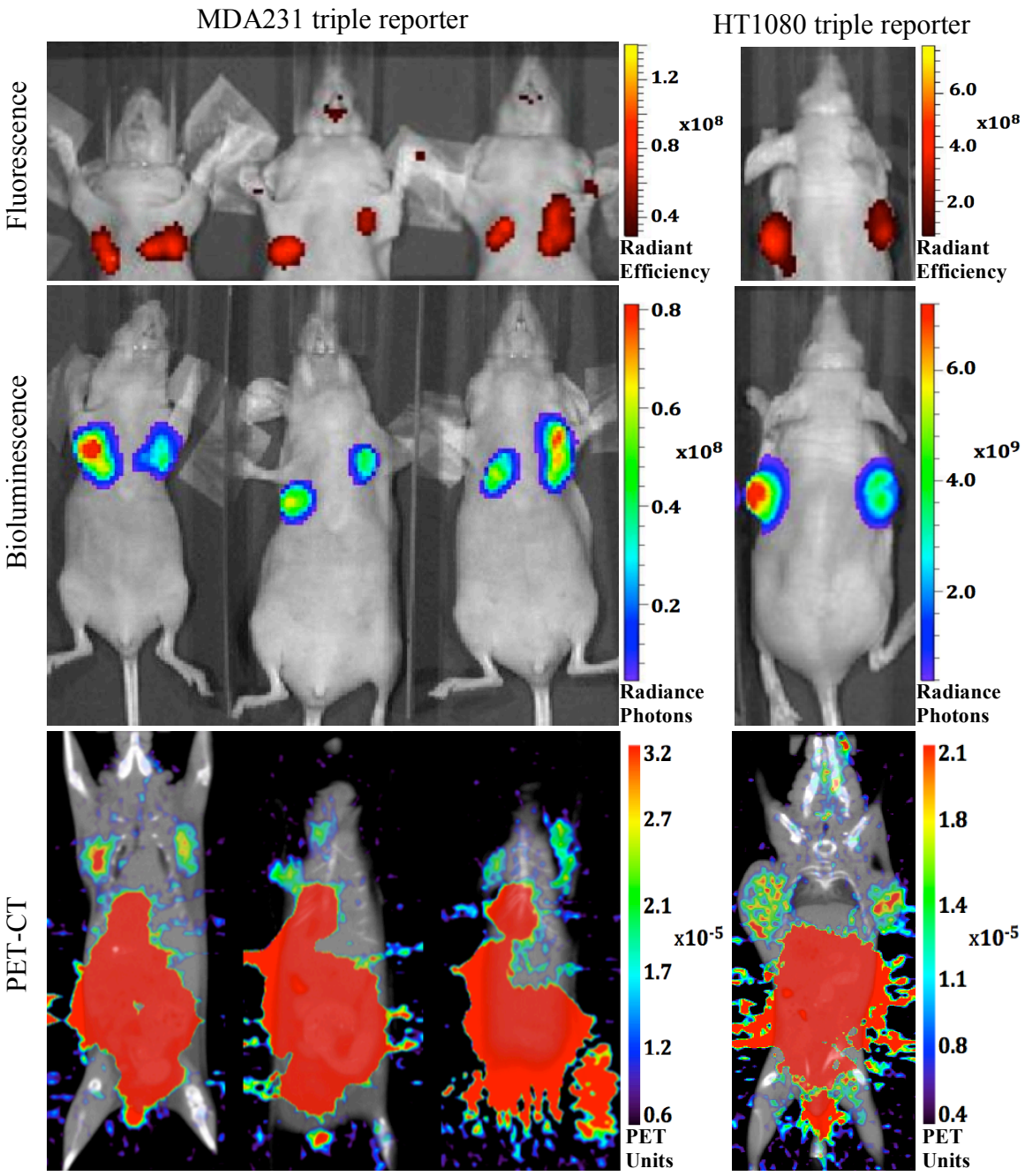

Figure 6. *In Vivo* Detection of Each Modality of the Triple Reporter Construct

Representative live animal images of three nu/nu mice with two MDA231 triple reporter FACS tumors per mouse and one nu/nu mouse with two HT1080 triple reporter FACS tumors confirm the activity of all three imaging modalities *in vivo*. The units of fluorescence radiant efficiency are emission light/excitation light, specifically $(p/s/cm^2/str)/(mW/cm^2)$. The units of bioluminescence radiance photons are $p/s/cm^2/sr$. The PET units are counts/s/voxel.

Table 1. Average Size and Average Total Fluorescence, Bioluminescence, and PET Signals of Triple Reporter FACS Tumors *In Vivo*

Only tumors that were detectable by all three modalities of the triple reporter construct were included in this dataset.

	MDA231 triple reporter FACS tumor average (n=8)	HT1080 triple reporter FACS tumor average (n=2)
Size measured by caliper (mm^3)	96.22 ± 42.08	339.00 ± 63.64
Size measured by PET-CT (mm^3)	126.00 ± 67.35	483.45 ± 52.31
Total fluorescence [(p/s)/(cm^2/sr)]	$3.56 \times 10^8 \pm 1.40 \times 10^8$	$1.61 \times 10^9 \pm 5.08 \times 10^8$
Total bioluminescence (p/s)	$2.99 \times 10^8 \pm 1.84 \times 10^8$	$2.73 \times 10^{10} \pm 9.80 \times 10^9$
Total PET (% bioavailable dose)	$9.76 \times 10^{-2} \pm 6.81 \times 10^{-2}$	$1.71 \times 10^{-1} \pm 4.93 \times 10^{-2}$

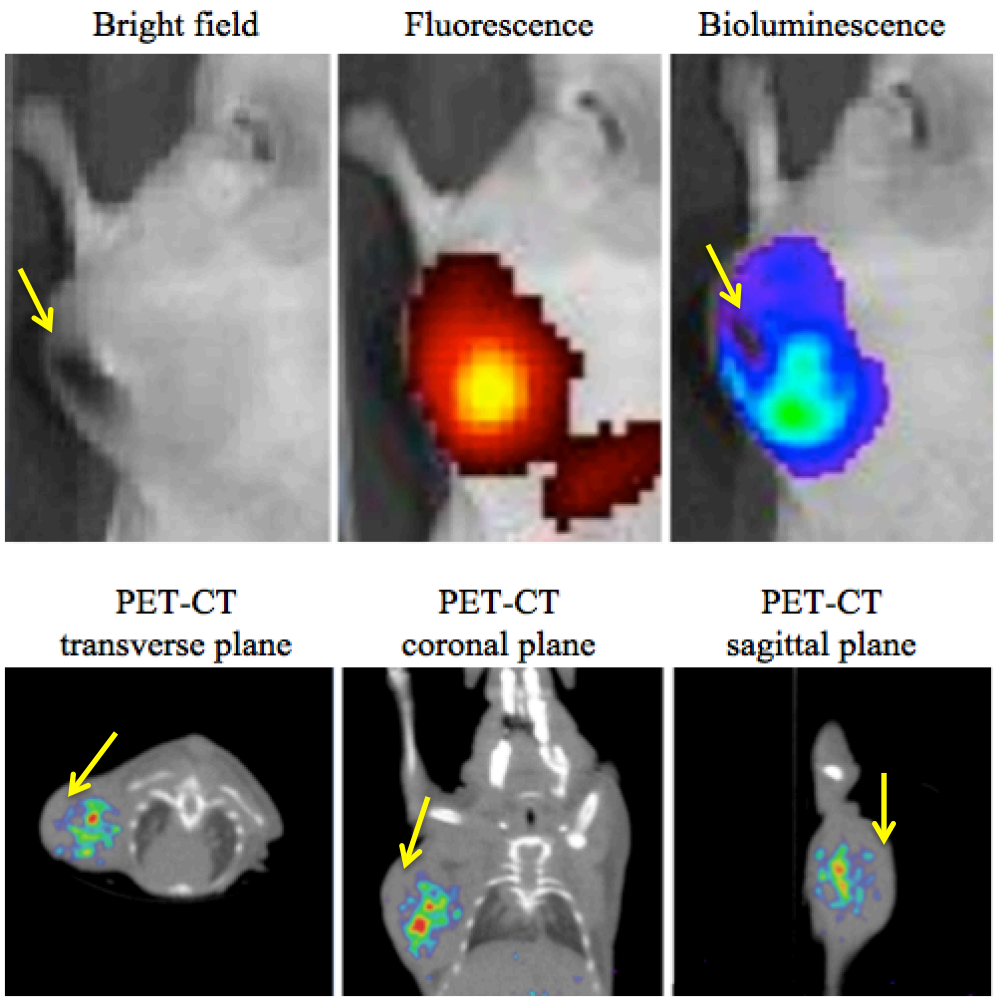

Figure 7. *In Vivo* Detection of Necrosis by Luc2 and Wttk Activity

A necrotic HT1080 triple reporter FACS tumor was imaged by fluorescence, bioluminescence, and PET-CT. Yellow arrows indicate detectable tumor regions with necrosis. Total bioluminescence signal and total PET signal of this tumor was significantly lower than in healthy HT1080 triple reporter FACS tumors.

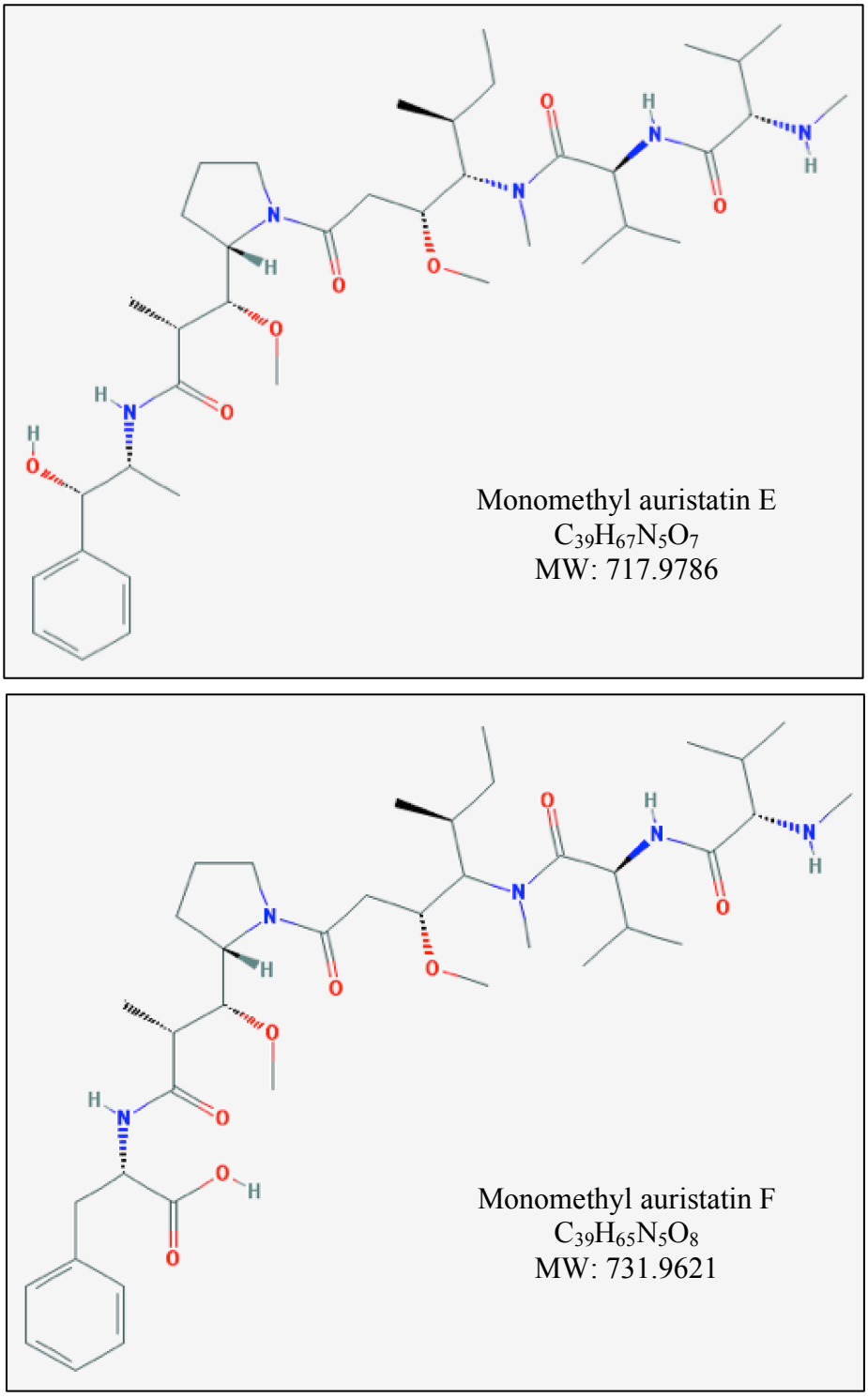

Figure 8. The Chemical Structures of MMAE and MMAF

MMAF has a charged C-terminal phenylalanine residue absent in MMAE. The chemical structures were downloaded from http://pubchem.ncbi.nlm.nih.gov/.

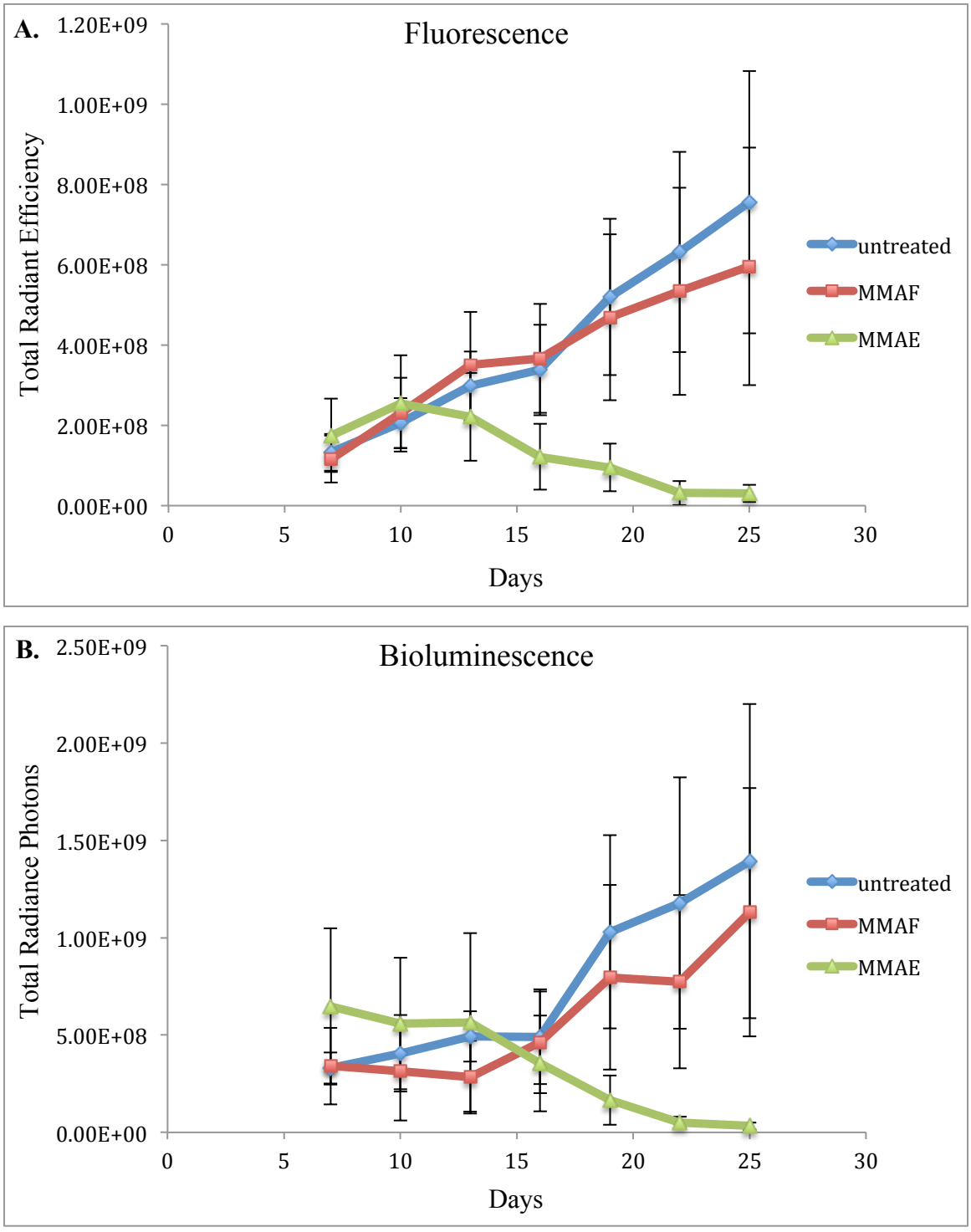

Figure 9. Quantified Therapeutic Responses of the MDA231 Triple Reporter FACS Tumors to MMAE and MMAF

(A) Average of the total fluorescence signal [(p/s)/(cm^2/sr)] of the tumors over time
(B) Average of the total bioluminescence signal (p/s) of the tumors over time

III:
Discussion

This thesis reports the successful cloning of an optimized triple modality reporter (Figure 1) and viral transduction of this triple reporter construct into two human cancer cell lines. Both transduced cell lines expressed all three modalities *in vitro* (Figures 2-4) and *in vivo* (Figure 6). Successful cleavage of viral 2A sequences allowed for proper protein folding and expression of each reporter gene product while achieving equal molarity of the reporter genes from transduction (Figure 4). This triple reporter was successfully used to quantify the therapeutic response of MDA231 human breast cancer tumors to MMAE and MMAF by fluorescence and bioluminescence optical imaging (Figure 9). MMAE has been shown to have >100x the potency of MMAF *in vitro* for a panel of cancer cell lines *(21)*. The results of the MMAE and MMAF therapy experiment with MDA231 tumors expressing the triple reporter *in vivo* confirm the published *in vitro* data. This validates the triple reporter as an accurate and valuable tool for imaging and quantifying tumor growth and regression. This is the first reported use of both fluorescence and bioluminescence signals from a multi-reporter construct to measure drug efficacy *in vivo*.

Currently, the standard method of measuring cancer growth and regression *in vivo* is the use of calipers (*23-25*). In fact, calipers have been used to evaluate all *in vivo* trials of antibody-conjugated MMAE and MMAF (*19-21, 26*). One issue with caliper measurements is that they generalize the tumor volume from measurements in two dimensions with the equation [0.5 x (largest diameter) x (smallest diameter)^2] (*23*). Caliper measurements can also be inconsistent or biased because calipers are manually tightened and loosened around the tumor to determine size, which is user dependent. Moreover, reliable caliper measurements require large palpable tumors; thus, the first

treatment does not start until the tumors have volumes of approximately 100 mm^3 (*21*). In the MMAE and MMAF therapy experiment, the tumors in the untreated group did not reach approximately 100 mm^3 based on caliper measurements until nineteen days after the injection of the cancer cells. With the triple reporter, therapy was initiated seven days after the injection of the cancer cells when the fluorescence and bioluminescence signals were both robust, allowing for earlier cancer treatment. Furthermore, calipers cannot be used to measure internal tumors, such as pancreatic tumors, making reporter constructs essential.

Another major shortcoming of the use of calipers is that caliper-based measurements do not incorporate the tumor health. Large tumors commonly have a necrotic core that is not obvious by visual inspection and not quantifiable by manual measurement. Similarly, tumors regressing due to drug treatments may die before they are cleared away. In this scenario, tumor cell death would predate a decrease in the tumor volume. The triple modality reporter is capable of detecting and quantifying tumor health with the bioluminescence and PET signals (Figure 7). As previously discussed, bioluminescence and PET imaging do not detect dead cells. Bioluminescence is produced when Luc2 catalyzes a reaction involving D-luciferin and ATP, resulting in release of a photon of light (*9*). PET signal is produced when wttk phosphorylates 18F-FHBG by transferring a phosphate group from ATP causing the radiolabeled probe to become trapped inside the cell (*11*). Necrotic and dead cells no longer produce ATP, which prevents the Luc2 and wttk reactions from occurring (*27, 28*). A decrease in the number of viable cells in a tumor reduces the overall activity of Luc2 and wttk in the tumor, diminishing bioluminescence and PET signals.

An improvement that could be made to the MDA231 triple reporter cell line and HT1080 triple reporter cell line is to select for the brightest individual clones instead of populations by FACS. The triple reporter FACS populations are comprised of a combination of the brightest transduced cells based on E2-Crimson fluorescence (Figure 2a), which allowed for stable expression of fluorescence over time. While the activity of the other two modalities was confirmed *in vitro* and *in vivo*, cells were never individually selected based on high expression of Luc2 or wttk as was done for E2-Crimson. Certain cells in the FACS populations may have significantly brighter or dimmer bioluminescence or PET signal than others, but because the FACS population was only tested as a whole for these two modalities, the dim cells were never excluded. Therefore, the triple reporter FACS populations consisted of brightly fluorescent cells with variable cell-to-cell expression of Luc2 and wttk. In this diverse population, some cells may have grown faster than others. Also, auristatin-based therapies target dividing cells (*19*); thus, the cells that were quiescent at the time of treatment were less affected. As a result, the bioluminescence and PET signals of triple reporter FACS tumors are not only representative of the overall tumor growth, but are also representative of the subset of cells in the population that had the fastest growth rate while also being the least targeted by auristatins.

This issue of uneven Luc2 expression in the triple reporter FACS populations is evident in the results of the MDA231 triple reporter FACS tumor therapy experiment. Fluorescence signal increased steadily over time in the untreated group, and the MMAE group had significant tumor regression after three doses (Figure 9a). However, while the bioluminescence signal did generally increase over time in the untreated group, it did not

do so as consistently and had relatively larger error bars for each data point. The added noise in the bioluminescence signal due to variable Luc2 expression in the MDA231 triple reporter FACS population caused measurements of tumor regression in the MMAE group to be statistically insignificant by bioluminescence signal until after four doses (Figure 9b).

Alternatively, individual clones of the triple reporter transduced cell lines could be selected by FACS and expanded in culture. Each FACS clone with high expression of E2-Crimson could then be tested for expression of Luc2 and wttk. The clone with the highest expression of all three modalities would be ideal for monitoring tumor growth and regression *in vivo*. This would increase the intensity and stability of reporter gene expression over time because all cells would theoretically have an equal growth rate and identical expression of each modality because all cells were derived from the same initial clone (*29*).

In summary, the development of cell lines expressing all three modalities of the optimized triple reporter allows for sensitive, long-term tracking of tumor growth *in vivo* by fluorescence, bioluminescence, and PET. This triple reporter improves on previous designs (*4*-*8*) by replacing the shorter wavelength eGFP (excitation 488 nm, emission 507 nm) or mRFP (excitation 584 nm, emission 607 nm) with E2-Crimson (excitation 611 nm, emission 648 nm) to increase fluorescence penetration through tissue. Also, previously chosen luciferases fLuc, hrl, and mtfl have been replaced by Luc2, which was codon optimized for increased expression in mammalian cells, allowing detection of single cells by bioluminescence. Additionally, self-cleaving viral 2A sequences separate

each component, which ensures equal stoichiometry of the reporter genes without requiring protein fusion or IRES sequences. The MMAE and MMAF therapy experiment in this thesis validates the optimized triple modality reporter as an accurate and quantifiable imaging tool *in vivo*. Based on these findings, applications of this triple reporter construct in other tumor growth models, for example tracking tumor metastasis, should be explored.

The optimized triple reporter would also be valuable for calibrating injectable imaging agents used in early tumor detection such as activatable cell-penetrating peptides (ACPPs). ACPPs are composed of a polyanionic domain with a protease-cleavable linker and a polycationic cell-penetrating peptide (CPP) covalently attached to a payload. The CPPs, often a sequence of consecutive arginines, can cross the cell membrane and can bring their payloads into mammalian cells without requiring specific receptors (*30, 31*). For early tumor detection with ACPPs, the cleavable linker is a specific cleavage sequence for a cancer-related protease and the payload is a fluorescent dye (*32*). Once cleaved, the fluorescent dye is brought into the cell by the CPP, resulting in fluorescently labeled cancer cells and defined tumor margins. Tumors can then be resected by fluorescent-guided surgery based on ACPP fluorescence signal (*33*). By using a cancer cell line expressing the optimized triple modality reporter, specificity of ACPPs to cancer cells could be quantified by overlaying the ACPP fluorescence signal with the triple reporter fluorescence signal. Furthermore, after fluorescent-guided surgery, the triple reporter could be used to monitor tumor recurrence by multiple modalities *in vivo*.

Finally, the triple reporter lentivirus is applicable to cancer gene therapy as well. Lentiviruses are important tools in gene therapy because of their ability to transfer genes

directly into the genomic DNA of dividing and non-dividing cells *in vivo* with long-term, stable expression (*34*). Lentiviral gene therapy with suicide genes delivers genes to cancer cells that can convert nontoxic prodrugs into active chemotherapeutic agents. One of the most commonly utilized suicide genes is HSV-1 thymidine kinase (*35, 36*). As demonstrated in Figure 4, only cells expressing wttk convert ganciclovir to a toxic triphosphate analog, which results in cell death (*22*). The optimized triple modality reporter lentivirus could be used in gene therapy to transduce tumors *in vivo* with the wttk suicide gene along with the E2-Crimson and Luc2 genes. Tumor regression due to lentiviral wttk/ganciclovir gene therapy could then be monitored and quantified by fluorescence, bioluminescence, and PET imaging.

IV:
Materials and Methods

Lentiviral Plasmid Cloning

Jin Yang, a lab technician in the Tsien lab, initially cloned the triple reporter construct into the pcDNA3.1/hygro+ vector (Life Technologies #V870-20). Trono Lab at Ecole Polytechnique Fédérale de Lausanne provided the second-generation lentiviral vector, second-generation psPAX2 lentiviral packaging plasmid, and pMDG.2 envelope plasmid.

The triple reporter was then cloned into a lentiviral viral vector using BamHI and EcoRI restriction sites. First, site directed mutagenesis was performed to remove the BamHI site between the Luc2 and wttk genes of the triple reporter construct in the pcDNA3.1/hygro+ vector. PCR primers were designed to change one base pair in the BamHI restriction site (5'-CCA AGA AGG GCG GCA AGA TCG CCG TGG GAT CTG GAG GTG GAT CTG GTG GCG GTG AGG-3' and 5'-CCT CAC CGC CAC CAG ATC CAC CTC CAG ATC CCA CGG CGA TCT TGC CGC CCT TCT TGG-3'). Next, a 50 µl PCR reaction was prepared with 250 ng vector, 20 nM concentration of each primer, and Phusion master mix (New England Biolabs #M0532S). The parameters for the 24 PCR cycles were denaturation for 1 minute at 98°C, hybridization for 30 seconds at 52°C, and extension for 4 minutes 30 seconds at 72°C. After completing PCR, 1 µl of Dpn1 (New England Biolabs) was added directly to the tube containing the PCR reaction and incubated for 1 hour and 30 minutes at 37°C to digest all methylated parent vector, leaving only the site-directed mutagenesis PCR product intact. For transformation of chemically competent cells with the PCR product, 50 µl of Oneshot TOP10 Chemically Competent E. coli Cells (Life Technologies #C-4040-03) were thawed on ice for 5 minutes. 3 µl of PCR product was added to the cells. The cells were

mixed by tapping gently and incubated on ice for 5 minutes. The cells were then heat shocked for 30 seconds at 42°C and immediately placed back on ice for 2 minutes. The transformed cells were spread on a pre-warmed LB agar plate containing 100 µg/ml ampicillin and grown overnight at 37°C to amplify the mutated triple reporter plasmid. The plasmid was purified by miniprep (Qiagen #27106), and the mutation in the BamHI restriction site between Luc2 and wttk genes was verified by a forward sequencing primer (5'-ACT GAC CGG CAA GTT GGA C-3').

Primers were designed to add the BamHI restriction site to the 5' end of the triple reporter construct (5'-AAA GGATCC GCC ACC ATG GAT AGC ACT GAG-3') and EcoRI restriction site to the 3' end of the triple reporter construct (5'-TTT GAATTC TCA GTT AGC CTC CCC CAT-3'). A 50 µl PCR reaction was prepared with 100 ng vector, 20 nM concentration of each primer, and Phusion master mix. The parameters for the 30 PCR cycles were denaturation for 10 seconds at 98°C, hybridization for 45 seconds at 57°C, and extension for 1 minute 45 seconds at 72°C. After completing PCR, 1 µl of Dpn1 (New England Biolabs) was added directly to the tube containing the PCR reaction and incubated for 1 hour and 30 minutes at 37°C to digest all methylated parent vector, leaving only the PCR product intact. The PCR product was run on a 1% agarose gel at 130 V for 25 minutes to isolate the triple reporter construct with added BamHI and EcoRI restriction sites, a single band of 3519 base pairs. This band was excised and gel purified using the QIAquick Gel Extraction Kit (Qiagen #28706).

1 µg of the triple reporter construct with added BamHI and EcoRI restriction sites and 1 µg of lentiviral vector were digested by EcoRI-HF and BamHI-HF restriction enzymes in NEBuffer 4 (New England Biolabs) for 30 minutes at 37°C. The digested

lentiviral vector was then dephosphorylated by 1 µl shrimp alkaline phosphatase (Roche) in a 20 µl reaction with dephosphorylation buffer (Roche) for 20 minutes at 37°C to prevent self-ligation. After dephosphorylation of the digested lentiviral vector, the digested lentiviral vector and digested triple reporter construct were concentrated with the DNA Clean & Concentrator Kit (Zymo Research #D4003). 20 ng vector and 50 ng triple reporter construct were ligated at room temperature for two hours by T4 DNA ligase (New England Biolabs) in a 20 µl reaction with T4 DNA Ligase Reaction Buffer (New England Biolabs). 50 µl of Oneshot TOP10 Chemically Competent E. coli Cells (Life Technologies) were transformed with 3 µl of ligation product as done before to amplify the viral vector containing the triple reporter. The plasmid was purified by maxiprep (Life Technologies #K2100-17).

Triple Reporter Lentivirus Production and Titration

The HEK293A packaging cell line was grown to 85% confluency in 6 15 cm tissue culture dishes in complete DMEM media (DMEM 4.5g/L glucose (Corning #10-013-CV), 10% FBS, 1% penicillin streptomycin). The media in the HEK293A cell dishes was then replaced with viral production media (DMEM 4.5g/L glucose, 5mM Sodium Butyrate, 1% penicillin streptomycin). 29.7 µl of 0.1M PEI (polyethylenimine) was added to 6 ml of Opti-MEM media (Life Technologies #31985-070) in a 15 ml tube and inverted to mix. 24 µg of triple reporter lentiviral plasmid, 45 µg of psPAX2 lentiviral packaging plasmid, and 30 µg of pMDG.2 envelope plasmid were added to 6 ml of Opti-MEM media in a 50 ml tube, inverted to mix, and left to sit at room temperature for 10 minutes. After 10 minutes, the PEI Opti-MEM solution was added

dropwise with agitation to the DNA Opti-MEM solution and incubated at room temperature for 15 minutes. Then, 2 ml of the combined solution was added dropwise to each HEK293A tissue culture dish. The cells were incubated at 37°C in a 5% CO_2 incubator for 10 hours. Media was aspirated and replaced with 17 ml viral production media per 15 cm dish and kept at 37°C in a 5% CO_2 incubator for 24 hours. Media was collected and stored at 4°C, then replaced with 17 ml viral production media per 15 cm dish and kept at 37°C in a 5% CO_2 incubator for 24 hours. Media was collected and combined with the stored media from the previous day. The media was sterilized through a 0.45 μm filter. 32 ml aliquots of sterilized media containing the triple reporter lentivirus were transferred into 6 38.5 ml thin wall centrifuge tubes (Beckman Coulter #344058). A sucrose gradient was created at the base of each tube with 2 ml of 20% sucrose in PBS. Tubes were centrifuged in a SW28 swinging bucket rotor (Beckman Coulter #342204) at 25,000 rpm 4°C with vacuum for 2 hours. Virus pellets were resuspended in a total of 300 μl sterile PBS and stored in 40 μl aliquots at -80°C.

Lentiviral Transduction of Human Cancer Cell Lines

MDA231 and HT1080 cancer cells were grown to 85% confluency in T25 tissue culture flasks in complete EMEM media (EMEM (ATCC #30-2003), 10% fetal bovine serum, 1% penicillin streptomycin). Media from each flask was replaced with 5 ml of viral production media without penicillin streptomycin. Each 1 ml of media was supplemented with 1 μl of 0.1M PEI. 40 μl of triple reporter lentivirus was added to each T25 flask and kept at 37°C in a 5% CO_2 incubator for 12 hours. Media was replaced with complete EMEM media. Cells were grown at 37°C in a 5% CO_2 incubator for 3 weeks.

Fluorescence Activated Cell Sorting (FACS)

3 weeks after transduction with the triple reporter lentivirus, E2-Crimson expression was observed in both cancer cell lines using an epifluorescence microscope with a 580/20 nm excitation filter and 653/95 nm emission filter. The top 1.5% brightest cells from the transduced HT1080 and MDA231 cell lines were collected by FACS with a 568 nm laser and 660/20 nm emission filter at 100 mW power. This brightly fluorescent FACS population was grown up for 3 weeks and frozen stocks were made. To freeze cells, 900 µl of 2x freeze solution (FBS + 15% DMSO) was aliquoted into a 2 ml cryovial. Approximately 2 x 10^6 cells were suspended in 900 µl complete EMEM media and added to the cryovial. The vial was frozen at -80°C for 2 to 6 days, then transferred to a liquid nitrogen freezer for long-term storage.

***In Vitro* Tests for Each Modality of the Triple Reporter in Transduced Cell Lines**

To prepare for epifluorescence imaging, the culture surfaces of a glass dishes were covered with a sterile 100 µg/ml solution of poly-d-lysine in water and incubated in a 5% CO_2 incubator at 37°C for 2 to 4 hours. Next, the poly-d-lysine solution was removed, and the culture surfaces were rinsed three times with PBS and dried. The triple reporter MDA231 FACS population and the triple reporter HT1080 FACS population were grown in the prepared glass dishes with complete EMEM for 2 days. After 2 days, media was aspirated and replaced with HBSS, and the cells were imaged on an epifluorescence microscope using a 580/20 nm excitation filter and 653/95 nm emission filter on the 40x oil objective with a 1 second exposure time.

Cells were then tested for bioluminescence activity. The triple reporter MDA231 FACS population, the triple reporter HT1080 FACS population, wild type MDA231 population, and wild type HT1080 population were each seeded in triplicate in a 48 well tissue culture plate. $7.4x10^4$ cells were added to each well. These cells were grown in complete EMEM at 37°C in a 5% CO_2 incubator for 24 hours, then their media was replaced with 100 µl of PBS. 30mg/ml stocks of D-luciferin potassium salt (In Vivo Imaging Solutions #10) were stored in amber centrifuge tubes at -80°C in the dark. A 30 mg/ml frozen stock was thawed and diluted to 750 µg/ml. 25ul (18.75 µg) was added to the 100 µl of PBS in each well, for a final D-luciferin working concentration of 150 µg/ml. Immediately after addition of D-luciferin, the plate was imaged with an IVIS Spectrum (FOV; C, binning; medium, f stop; 1, exposure time; auto) (Caliper Life Sciences). Bioluminescence signal was quantified with Living Image software (Caliper Life Sciences).

Lastly, wttk activity was confirmed. The triple reporter MDA231 FACS population, the triple reporter HT1080 FACS population, wild type MDA231 population, and wild type HT1080 population were each seeded in triplicate in a 48 well tissue culture plate. $4x10^3$ cells were added to each well. Each group of three wells for each population was treated with a different dose of ganciclovir (InvivoGen #sud-gcv) in complete EMEM: 0 µg/ml, 1 µg/ml, 10 µg/ml. The cells were grown at 37°C in a 5% CO_2 incubator for 6 days. Cells were visually observed with a white light microscope to check for cell death by ganciclovir treatment. Then, cell death by ganciclovir treatment was quantified using the CellTiter 96® AQueous One Solution Cell Proliferation Assay (Promega #G3582). Results of this colorimetric method for determining live cell count

were collected using an Infinite M1000 PRO plate reader (Tecan) measuring absorbance at 490 nm in bottom read mode.

Western Blot for Each Modality of the Triple Reporter in Transduced Cell Lines

3 x 10^4 cells from the triple reporter MDA231 FACS population, the triple reporter HT1080 FACS population, wild type MDA231 population, and wild type HT1080 population were each centrifuged at 90 g for 5 minutes. Each cell pellet was lysed in 100 µl of 1x RIPA buffer (Cell Signaling Technology #9806) with 0.5% SDS and protease inhibitors (Roche #11 873 580 001) by pipetting, vortexing, and freeze thawing. A volume equivalent to 1.5 x 10^3 lysed cells was reduced and denatured in NuPage LDS Sample Buffer (Life Technologies #NP0007) with 8% BME at 95°C for 5 minutes. The samples were run next to the Precision Plus Duel Color Standards (Bio-Rad #161-0374) at in a 4-12% Bis-Tris polyacrylamide gel (Life Technologies NP0323BOX) at 150V for 1 hour and 15 minutes. The gel was then transferred to a nitrocellulose membrane in buffer TG (25mM Ultrapure Tris, pH 8.3, and 192mM glycine) with 20% ethanol in an XCell II Blot Module (Invitrogen #EI9051) at 30V for 1 hour and 20 minutes.

The membrane was blocked for 1 hour at room temperature on a shaking platform in TBST (50 mM Tris, 150 mM NaCl, 0.1% Tween 20, adjusted to pH 7.6 with HCl) with 10% donkey serum (Gemini Bio-products #100-150). The membrane was incubated in primary antibody diluted in TBST with 10% donkey serum overnight at 4°C. The primary antibody dilutions for each modality and a loading control were as follows: 1:250 anti HSV-1 thymidine kinase goat polyclonal (Santa Cruz Biotechnology #sc-

28038), 1:3000 anti DsRed rabbit polyclonal (Clonetech #632496), 1:3000 anti firefly luciferase mouse monoclonal (Abcam ab16466), 1:5000 anti GAPDH rabbit polyclonal (Sigma-Aldrich #G9545).

The membrane was washed 4 times in 20 ml TBST with 5 min incubation in each wash on a room temperature shaking platform. The membrane was incubated in secondary antibody diluted in TBST with 5% donkey serum for 1 hour. Secondary antibody dilutions were as follows: 1:2500 donkey anti-goat IgG HRP conjugate (Promega #V8051), 1:3000 goat anti-rabbit IgG HRP conjugate (Cell Signaling Technologies #7074), 1:3000 goat anti-mouse IgG HRP conjugate (Bio-Rad #170-6516).

The membrane was washed 4 times in 20 ml TBST with 5 minutes incubation in each wash on a room temperature shaking platform. The membrane was then incubated in 8 ml of chemiluminescent substrate (Thermo Scientific PI34080) for 1 minute on a room temperature shaking platform.

The membrane was exposed to film in a dark room and developed. After, the membrane was washed in 10 ml TBST and stripped with 5 ml Western blot stripping buffer (Thermo Scientific #21059). The membrane was washed twice in 10 ml TBST with a 5 minute incubation in each wash on a room temperature shaking platform. The membrane was reprobed with the next primary antibody. This was repeated for detection of each reporter protein as well as for the loading control GAPDH.

In Vivo Tests for Each Modality of the Triple Reporter in Transduced Cell Lines

50 µl injections of triple reporter MDA231 cells were prepared by suspending 1 x 10^6 cells in 25 µl dPBS and mixing with 25 µl of 8.9 mg/ml cold matrigel on ice. 6-week

old female nu/nu mice were injected orthotopically in the mammary fat pads with triple reporter MDA231 cells. 2 tumors were grown in each mouse for 2 weeks.

50 µl injections of triple reporter HT1080 cells were prepared by suspending 5 x 10^5 cells in 50 µl dPBS. 6-week old female nu/nu mice were injected subcutaneously at the shoulder blades with triple reporter HT1080 cells. 2 tumors were grown in each mouse for 2 weeks.

High gut retention is characteristic of 18F-FHBG, requiring that tumors be placed away from the abdomen of each mouse.

Whole body fluorescence and bioluminescence was imaged using an IVIS Spectrum with 2.5% isoflurane anesthesia. Fluorescence background was imaged with a 465 nm excitation filter and a 660 nm emission filter (FOV; D, binning; medium, f stop; 2, exposure time; 1 second). E2-Crimson fluorescence was imaged with a 605 nm excitation filter and a 660 nm emission filter (FOV; D, binning; medium, f stop; 2, exposure time; auto). Fluorescent background was subtracted and total radiant efficiency was quantified using Living Image software. Bioluminescence background was imaged with excitation filter blocked and emission filter open (FOV; D, binning; medium, f stop; 1, exposure time; 1 second). D-luciferin was prepared at 15 mg/ml in dPBS. Mice were injected subcutaneously on the flank with 10 µl of the 15 mg/ml D-luciferin solution per gram of mouse. 15 minutes after injection, mice were imaged with excitation filter blocked and emission filter open (FOV; D, binning; medium, f stop; 1, exposure time; auto). Total radiance photons were quantified using Living Image software.

Tumors were imaged for PET-CT with a microPET scanner (Siemens) and a microCAT II system (ImTek) by the David Stout laboratory at the Crump Institute for

Molecular Imaging, UCLA. Approximately 150 μCi of 18F-FHBG, synthesized by the Stout lab, were intravenously administered per mouse and allowed 2 hours to circulate before imaging. Background % bioavailable dose of 18F-FHBG in wild type tumors and % bioavailable dose of 18F-FHBG in triple reporter tumors were quantified using AMIDE software.

Quantifying Cancer Therapy *In Vivo* with the Triple Reporter Construct

5-week old female nu/nu mice were injected with 7.5×10^5 triple reporter MDA231 cells per tumor in matrigel. 2 tumors were grown orthotopically and bilaterally in the mammary fat pads of each mouse. After 7 days, mice were randomized into 3 treatment groups (untreated, MMAE, MMAF) with 5 mice per group for a total of 10 tumors per group. Mice were treated with a dose of 0.5 nmol of drug per gram of mouse every 3 days with a total of 6 doses. Whole body fluorescence and bioluminescence images were captured with an IVIS Spectrum as described previously. Total tumor fluorescence and bioluminescence signals were quantified using Living Image software, and tumor signals were averaged within groups. Tumor size was also measured using millimeter calipers starting on day 10 when tumors were somewhat more reliably palpable. Mouse weight was recorded throughout the experiment.

References

(1) Massoud, T. F., and Gambhir, S. S. (2003) Molecular imaging in living subjects: seeing fundamental biological processes in a new light. *Genes Dev 17*, 545-80.

(2) Ormo, M., Cubitt, A. B., Kallio, K., Gross, L. A., Tsien, R. Y., and Remington, S. J. (1996) Crystal structure of the Aequorea victoria green fluorescent protein. *Science 273*, 1392-5.

(3) Cubitt, A. B., Heim, R., Adams, S. R., Boyd, A. E., Gross, L. A., and Tsien, R. Y. (1995) Understanding, improving and using green fluorescent proteins. *Trends Biochem Sci 20*, 448-55.

(4) Ray, P., De, A., Min, J. J., Tsien, R. Y., and Gambhir, S. S. (2004) Imaging tri-fusion multimodality reporter gene expression in living subjects. *Cancer Res 64*, 1323-30.

(5) Ponomarev, V., Doubrovin, M., Serganova, I., Vider, J., Shavrin, A., Beresten, T., Ivanova, A., Ageyeva, L., Tourkova, V., Balatoni, J., Bornmann, W., Blasberg, R., and Gelovani Tjuvajev, J. (2004) A novel triple-modality reporter gene for whole-body fluorescent, bioluminescent, and nuclear noninvasive imaging. *Eur J Nucl Med Mol Imaging 31*, 740-51.

(6) Kesarwala, A. H., Prior, J. L., Sun, J., Harpstrite, S. E., Sharma, V., and Piwnica-Worms, D. (2006) Second-generation triple reporter for bioluminescence, micro-positron emission tomography, and fluorescence imaging. *Mol Imaging 5*, 465-74.

(7) Ray, P., Tsien, R., and Gambhir, S. S. (2007) Construction and validation of improved triple fusion reporter gene vectors for molecular imaging of living subjects. *Cancer Res 67*, 3085-93.

(8) Ibrahimi, A., Vande Velde, G., Reumers, V., Toelen, J., Thiry, I., Vandeputte, C., Vets, S., Deroose, C., Bormans, G., Baekelandt, V., Debyser, Z., and Gijsbers, R. (2009) Highly efficient multicistronic lentiviral vectors with peptide 2A sequences. *Hum Gene Ther 20*, 845-60.

(9) Gould, S. J., and Subramani, S. (1988) Firefly luciferase as a tool in molecular and cell biology. *Anal Biochem 175*, 5-13.

(10) Kim, J. B., Urban, K., Cochran, E., Lee, S., Ang, A., Rice, B., Bata, A., Campbell, K., Coffee, R., Gorodinsky, A., Lu, Z., Zhou, H., Kishimoto, T. K., and Lassota, P. (2010) Non-invasive detection of a small number of bioluminescent cancer cells in vivo. *PLoS One 5*, e9364.

(11) Blasberg, R. (2002) PET imaging of gene expression. *Eur J Cancer 38*, 2137-46.

(12) Jackson, R. J. (1988) RNA translation. Picornaviruses break the rules. *Nature 334*, 292-3.

(13) Szymczak, A. L., and Vignali, D. A. (2005) Development of 2A peptide-based strategies in the design of multicistronic vectors. *Expert Opin Biol Ther 5*, 627-38.

(14) Donnelly, M. L., Luke, G., Mehrotra, A., Li, X., Hughes, L. E., Gani, D., and Ryan, M. D. (2001) Analysis of the aphthovirus 2A/2B polyprotein 'cleavage' mechanism indicates not a proteolytic reaction, but a novel translational effect: a putative ribosomal 'skip'. *J Gen Virol 82*, 1013-25.

(15) Bukrinsky, M. I., Haggerty, S., Dempsey, M. P., Sharova, N., Adzhubel, A., Spitz, L., Lewis, P., Goldfarb, D., Emerman, M., and Stevenson, M. (1993) A nuclear localization signal within HIV-1 matrix protein that governs infection of non-dividing cells. *Nature 365*, 666-9.

(16) Amado, R. G., and Chen, I. S. (1999) Lentiviral vectors--the promise of gene therapy within reach? *Science 285*, 674-6.

(17) Kim, T. K., and Eberwine, J. H. (2010) Mammalian cell transfection: the present and the future. *Anal Bioanal Chem 397*, 3173-8.

(18) Charrier, S., Ferrand, M., Zerbato, M., Precigout, G., Viornery, A., Bucher-Laurent, S., Benkhelifa-Ziyyat, S., Merten, O. W., Perea, J., and Galy, A. (2011) Quantification of lentiviral vector copy numbers in individual hematopoietic colony-forming cells shows vector dose-dependent effects on the frequency and level of transduction. *Gene Ther 18*, 479-87.

(19) Doronina, S. O., Toki, B. E., Torgov, M. Y., Mendelsohn, B. A., Cerveny, C. G., Chace, D. F., DeBlanc, R. L., Gearing, R. P., Bovee, T. D., Siegall, C. B., Francisco, J. A., Wahl, A. F., Meyer, D. L., and Senter, P. D. (2003) Development of potent monoclonal antibody auristatin conjugates for cancer therapy. *Nat Biotechnol 21*, 778-84.

(20) Doronina, S. O., Bovee, T. D., Meyer, D. W., Miyamoto, J. B., Anderson, M. E., Morris-Tilden, C. A., and Senter, P. D. (2008) Novel peptide linkers for highly potent antibody-auristatin conjugate. *Bioconjug Chem 19*, 1960-3.

(21) Doronina, S. O., Mendelsohn, B. A., Bovee, T. D., Cerveny, C. G., Alley, S. C., Meyer, D. L., Oflazoglu, E., Toki, B. E., Sanderson, R. J., Zabinski, R. F., Wahl, A. F., and Senter, P. D. (2006) Enhanced activity of monomethylauristatin F through monoclonal antibody delivery: effects of linker technology on efficacy and toxicity. *Bioconjug Chem 17*, 114-24.

(22) Cannon, J. S., Hamzeh, F., Moore, S., Nicholas, J., and Ambinder, R. F. (1999) Human herpesvirus 8-encoded thymidine kinase and phosphotransferase homologues confer sensitivity to ganciclovir. *J Virol 73*, 4786-93.

(23) Steiner, J. L., Davis, J. M., McClellan, J. L., Enos, R. T., and Murphy, E. A. (2013) Effects of voluntary exercise on tumorigenesis in the C3(1)/SV40Tag transgenic mouse model of breast cancer. *Int J Oncol 42*, 1466-72.

(24) Riwanto, I., Budijitno, S., Dharmana, E., Handojo, D., Prasetyo, S. A., Eko, A., Suseno, D., and Prasetyo, B. (2011) Effect of phaleria macrocarpa supplementation on apoptosis and tumor growth of C3H mice with breast cancer under treatment with adriamycin-cyclophosphamide. *Int Surg 96*, 164-70.

(25) Young, E., Miele, L., Tucker, K. B., Huang, M., Wells, J., and Gu, J. W. (2010) SU11248, a selective tyrosine kinases inhibitor suppresses breast tumor angiogenesis and growth via targeting both tumor vasculature and breast cancer cells. *Cancer Biol Ther 10*, 703-11.

(26) Jackson, D., Gooya, J., Mao, S., Kinneer, K., Xu, L., Camara, M., Fazenbaker, C., Fleming, R., Swamynathan, S., Meyer, D., Senter, P. D., Gao, C., Wu, H., Kinch, M., Coats, S., Kiener, P. A., and Tice, D. A. (2008) A human antibody-drug conjugate targeting EphA2 inhibits tumor growth in vivo. *Cancer Res 68*, 9367-74.

(27) Petty, R. D., Sutherland, L. A., Hunter, E. M., and Cree, I. A. (1995) Comparison of MTT and ATP-based assays for the measurement of viable cell number. *J Biolumin Chemilumin 10*, 29-34.

(28) Kuruppu, D., Brownell, A. L., Zhu, A., Yu, M., Wang, X., Kulu, Y., Fuchs, B. C., Kawasaki, H., and Tanabe, K. K. (2007) Positron emission tomography of herpes simplex virus 1 oncolysis. *Cancer Res 67*, 3295-300.

(29) Christoph, S., Schlegel, J., Alvarez-Calderon, F., Kim, Y. M., Brandao, L. N., DeRyckere, D., and Graham, D. K. (2013) Bioluminescence imaging of leukemia cell lines in vitro and in mouse xenografts: effects of monoclonal and polyclonal cell populations on intensity and kinetics of photon emission. *J Hematol Oncol 6*, 10.

(30) Jiang, T., Olson, E. S., Nguyen, Q. T., Roy, M., Jennings, P. A., and Tsien, R. Y. (2004) Tumor imaging by means of proteolytic activation of cell-penetrating peptides. *Proc Natl Acad Sci U S A 101*, 17867-72.

(31) Whitney, M., Savariar, E. N., Friedman, B., Levin, R. A., Crisp, J. L., Glasgow, H. L., Lefkowitz, R., Adams, S. R., Steinbach, P., Nashi, N., Nguyen, Q. T., and Tsien, R. Y. (2013) Ratiometric activatable cell-penetrating peptides provide rapid in vivo readout of thrombin activation. *Angew Chem Int Ed Engl 52*, 325-30.

(32) Savariar, E. N., Felsen, C. N., Nashi, N., Jiang, T., Ellies, L. G., Steinbach, P., Tsien, R. Y., and Nguyen, Q. T. (2013) Real-time in vivo molecular detection of primary tumors and metastases with ratiometric activatable cell-penetrating peptides. *Cancer Res 73*, 855-64.

(33) Nguyen, Q. T., Olson, E. S., Aguilera, T. A., Jiang, T., Scadeng, M., Ellies, L. G., and Tsien, R. Y. (2010) Surgery with molecular fluorescence imaging using activatable cell-penetrating peptides decreases residual cancer and improves survival. *Proc Natl Acad Sci U S A 107*, 4317-22.

(34) Zufferey, R., Nagy, D., Mandel, R. J., Naldini, L., and Trono, D. (1997) Multiply attenuated lentiviral vector achieves efficient gene delivery in vivo. *Nat Biotechnol 15*, 871-5.

(35) Leinonen, H. M., Ruotsalainen, A. K., Maatta, A. M., Laitinen, H. M., Kuosmanen, S. M., Kansanen, E., Pikkarainen, J. T., Lappalainen, J. P., Samaranayake, H., Lesch, H. P., Kaikkonen, M. U., Yla-Herttuala, S., and Levonen, A. L. (2012) Oxidative stress-regulated lentiviral TK/GCV gene therapy for lung cancer treatment. *Cancer Res 72*, 6227-35.

(36) Tian, D., Sun, Y., Yang, Y., Lei, M., Ding, N., and Han, R. (2013) Human telomerase reverse-transcriptase promoter-controlled and herpes simplex virus thymidine kinase-armed adenoviruses for renal cell carcinoma treatment. *Onco Targets Ther 6*, 419-26.